Published in final edited form as:

Genes Brain Behav. 2014 March ; 13(3): 261–275. doi:10.1111/gbb.12119.

Quantitative trait loci mapping and gene network analysis implicate protocadherin-15 as a determinant of brain serotonin transporter expression

R. Ye[†], **A. M. D. Carneiro**[†], **Q. Han**[†], **D. Airey**[†], **E. Sanders-Bush**[†], **B. Zhang**[‡], **L. Lu**[§], **R. Williams**[§], and **R. D. Blakely**[*,†,¶]

[†]Department of Pharmacology, Vanderbilt University School of Medicine, Nashville

[‡]Department of Biomedical Informatics, Vanderbilt University School of Medicine, Nashville

[§]Department of Anatomy and Neurobiology, University of Tennessee Health Science Center, Memphis

[¶]Department of Psychiatry, Vanderbilt University School of Medicine, Nashville, TN, USA

Abstract

Presynaptic serotonin (5-hydroxytryptamine, 5-HT) transporters (SERT) regulate 5-HT signaling via antidepressant-sensitive clearance of released neurotransmitter. Polymorphisms in the human SERT gene (*SLC6A4*) have been linked to risk for multiple neuropsychiatric disorders, including depression, obsessive-compulsive disorder and autism. Using BXD recombinant inbred mice, a genetic reference population that can support the discovery of novel determinants of complex traits, merging collective trait assessments with bioinformatics approaches, we examine phenotypic and molecular networks associated with SERT gene and protein expression. Correlational analyses revealed a network of genes that significantly associated with SERT mRNA levels. We quantified SERT protein expression levels and identified region- and gender-specific quantitative trait loci (QTLs), one of which associated with male midbrain SERT protein expression, centered on the protocadherin-15 gene (*Pcdh15*), overlapped with a QTL for midbrain 5-HT levels. *Pcdh15* was also the only QTL-associated gene whose midbrain mRNA expression significantly associated with both SERT protein and 5-HT traits, suggesting an unrecognized role of the cell adhesion protein in the development or function of 5-HT neurons. To test this hypothesis, we assessed SERT protein and 5-HT traits in the *Pcdh15* functional null line (*Pcdh15*$^{av\text{-}3J}$), studies that revealed a strong, negative influence of *Pcdh15* on these phenotypes. Together, our findings illustrate the power of multidimensional profiling of recombinant inbred lines in the analysis of molecular networks that support synaptic signaling, and that, as in the case of *Pcdh15*, can reveal novel relationships that may underlie risk for mental illness.

Keywords

Antidepressant; BXD; microarray; network; protocadherin; QTL; serotonin; SLC5A7; SLC6A4; SLC6A3; TPH2; transcriptome; transporter; VMAT2

[*]Corresponding author: R. D. Blakely, PhD, Suite 7140 MRBIII, Vanderbilt University School of Medicine, 465 21st Avenue South, Nashville, TN 37232-8548, USA. randy.blakely@vanderbilt.edu.

The biogenic indoleamine serotonin (5-hydroxytryptamine, 5-HT) plays key roles as a modulator of central nervous system (CNS) and periphery physiology (Azmitia 2007; Berger *et al.* 2009). In the brain, 5-HT-secreting projections originate from midbrain and brainstem raphe nuclei, terminating both locally and distally at virtually every level of the neuraxis. 5-Hydroxytryptamine signaling at serotonergic synapses is terminated by efficient clearance of released neurotransmitter, mediated by the 5-HT transporter (*SLC6A4*, SERT) (Blakely *et al.* 1991; Hoffman *et al.* 1991; Ramamoorthy *et al.* 1993). SERT is a target of important psychoactive substances including cocaine and 3,4-methylenedioxy-N-methamphetamine (MDMA, 'ecstasy'), as well as of the selective 5-HT reuptake inhibitors (SSRIs) and non-selective serotonin–norepinephrine reuptake inhibitors (SNRIs), medications that are widely prescribed for the treatment of major depression, anxiety disorders and obsessive-compulsive disorder (OCD).

Given the essential roles that SERT plays in regulating synaptic 5-HT levels, as well as recycling 5-HT for reuse, it is not surprising that alterations in SERT expression and/or activity can impact behavior as well as risk for behavioral disorders. For example, the *SLC6A4* gene possesses promoter sequence variation (5HTTLPR) that has been reported to influence SERT mRNA and protein expression as well as risk for behavioral disorders (Homberg & Lesch 2011; Lesch *et al.* 1996). Additionally, functional *SLC6A4* coding variation has been identified in subjects with OCD (Ozaki *et al.* 2003; Voyiaziakis *et al.* 2011) and autism (Sutcliffe *et al.* 2005).

The impact of SERT on physiology and behavior has also been well demonstrated in rodent models that lack or overexpress the *Slc6a4* gene [reviewed in (Murphy *et al.* 2008) and (Kalueff *et al.* 2010)]. We recently reported studies of a KI mouse model that expresses an autism-associated SERT coding variant (Ala56). In these mice, SERT-mediated 5-HT clearance is constitutively elevated in vivo, leading to elevation of whole-blood 5-HT levels (hyperserotonemia), an autism biomarker, and increased repetitive behavior, as well as communication and social behavior deficits (Veenstra-VanderWeele *et al.* 2012). Interestingly, SERT proteins differ by two amino acids in C57BL/6J vs. DBA/2J (or 129S6) lines, variation that impacts SERT function and associates with multiple biochemical, anatomical and behavioral traits (Carneiro *et al.* 2009; Ye & Blakely 2011).

The significant contribution of SERT in the control of 5-HT signaling, behavior and mental illness compels a detailed understanding of mechanisms by which the transporter is regulated, and how this regulation supports behavior and disease. Unbiased approaches, particularly those that permit multidimensional profiling, offer opportunities to establish novel, molecular and phenotypic relationships. One such approach involves the use of recombinant inbred mouse lines, such as those generated from a cross of C57BL/6J and DBA/2J parents (BXD) (Andreux *et al.* 2012; Mozhui *et al.* 2010). The full sequencing of the parental strains, along with thousands of archived phenotypes, has resulted in a powerful resource by which BXD strain variation can be used to elucidate molecular and phenotypic networks.

In a recent report (Ye *et al.* 2014), we quantified midbrain mRNAs in BXD lines, as well as tissue levels of 5-HT, 5-hydroxyindoleacetic acid (5-HIAA) and 5-HT turnover, and used *in silico* approaches to nominate novel genes that may contribute to these measures. In this study, we describe our efforts to profile SERT mRNA and protein levels in the same BXD lines, studies that revealed distinct, molecular networks that associate with either trait. Additionally, we describe how the mapping of genomic loci associated with SERT protein levels converged with our prior studies of quantitative trait loci (QTLs) linked to 5-HT homeostasis through the common identification of the *Pcdh15*. Lastly, we detail our efforts to validate a role of *Pcdh15* in SERT expression and 5-HT homeostasis using *Pcdh15* null mice.

Materials and methods

Animals and genotyping

All studies with mice were performed under approved protocols of the Institutional Animal Care and Use Committees of the Oak Ridge National Laboratory and Vanderbilt University. Animals were housed on a 12:12 light:dark cycle with lights on at 0600 h and food and water provided *ad libitum*. A total of 126 BXD recombinant inbred mice from 38 strains were used. There were 34 strains of males (30 strains with two animals per strain and 4 strains with single animal) and 29 strains of females (26 strains with two animals per strain and 3 strains with single animal). The average age of the mice was 74 days (range: 51–89 days). A total of 67 male mice and 59 female mice were used in our studies (Table S1). Females were used irrespective of estrous cycle though they were never exposed to males or male bedding after weaning, typically required to initiate synchronized estrous cycling. Midbrain and diencephalon (thalamus and hypothalamus) were dissected on ice from mice killed by rapid decapitation. Midbrain was defined as brain tissue lying between the anterior and posterior margins of the inferior and superior colliculi, respectively (AP approximately −3.25 to −5.02 mm relative to bregma). Hypothalamus and thalamus were defined according to the Paxinos and Watson Atlas of the Mouse Brain (AP approximately −0.80 to −3.25 mm relative to bregma) (Watson & Paxinos 2010). Tissues were frozen on dry ice and stored at −80°C prior to high-performance liquid chromatography (HPLC) analysis for biogenic amines and protein extraction. *Pcdh15*$^{av\text{-}3J}$ mice were obtained from Jackson Labs (stock number: 002072). Mouse genotyping was performed using genomic DNA extracted from tail clips using the Extract-N-AMP tissue PCR Kit (Sigma, St. Louis, MO, USA) according to the manufacturer's instructions. Genotyping was performed by polymerase chain reaction (PCR) with oligonucleotides 5′ GAC GGC AAA CTG CTC GAT A (RB3964) and 5′ GGG ATG CAA CAG AGA TGA T (RB3965) and was based on a single nucleotide addition in the *Pcdh15*$^{av\text{-}3J}$ allele that introduces an *MboII* restriction site. Genotypes were determined by the size of *MboII* digested PCR products (+/+: 190 bp; +/*av-3J*: 190, 120 and 70 bp; *av-3J/av-3J*: 120 and 70 bp), as determined by agarose gel electrophoresis.

Brain tissue neurochemical measurements

For assessment of 5-HT and 5-HIAA levels in wild-type (WT) and *Pcdh15*$^{av\text{-}3J}$ mice, tissues were homogenized using an Omni Tissue Homogenizer (Omni International, Kennesaw, GA, USA) in 100–750 μl of 0.1 M trichloroacetic acid (TCA), 10 mM sodium acetate, 0.1 mM

ethylenediaminetetraacetic acid (EDTA), 5 ng/ml isoproterenol (as internal standard) and 10.5% methanol (pH 3.8). 5-Hydroxytryptamine and 5-HIAA were determined by HPLC through the Neurochemistry Core of the Vanderbilt Brain Institute, utilizing an Antec Decade II (oxidation: 0.5) electrochemical detector (Antec LLC, Boston, MA, USA) operated at 33°C. Twenty microliter samples of the supernatant were injected using a Waters 717+ autosampler (Waters, Milford, MA, USA) onto a Phenomenex Nucleosil (5u, 100A) C18 HPLC Column (150 × 4.60 mm^2) (Phenomenex, Torrance, CA, USA). Samples were eluted with a mobile phase consisting of 89.5% 0.1 M TCA, 10 mM sodium acetate, 0.1 mM EDTA and 10.5% methanol (pH 3.8). Solvent was delivered at 0.6 ml/min using a Waters 515 HPLC Pump. HPLC control and data acquisition were managed by Millennium 32 software.

Western blotting and quantification

After HPLC biogenic amine measurements, tissue protein pellets were solubilized with 250 μl RIPA buffer [50 mM Tris, pH 7.4, 150 mM NaCl, 1 mM EDTA, 1% Triton X-100, 1% sodium deoxycholate and 0.1% sodium dodecyl sulfate (SDS)] containing protease inhibitors (1:100; Sigma). Protein concentrations were determined by the bicinchoninic acid (BCA) method (Pierce, Thermo Fisher Scientific, Rockford, IL, USA). Equal amounts of extracted supernatants were separated by 10% SDS-polyacrylamide gel electrophoresis on a Bio-Rad Mini-PROTEAN 3 Dodeca Cell (Bio-rad, Herules, CA, USA), transferred to PVDF membranes and immunoblotted using SERT primary antibody (Calbiochem: Pc177L; 1:5000, Merck KGaA, Darmstadt, Germany) and mouse anti-rabbit secondary antibody (Jackson ImmunoResearch: 211-035-109; 1:10 000, West Grove, PA, USA). We chose this particular SERT antibody, which targets the SERT C-terminus of SERT, as BXD strains differ by the expression of N-terminal SERT coding variation [Gly39 arising from the C57BL/6J allele and Glu39 arising from the DBA/2J allele (Carneiro *et al.* 2009)]. Immunoreactive bands corresponding to SERT (absent in SERT KO mice) were identified by chemiluminescence (Western Lightning ECL Pro, Perkin Elmer, Waltham, MA, USA) and X-ray film (Biomax MS, Kodak, 8294985, Rochester, NY, USA) exposure. Optical densities of bands were quantified using ImageJ software 1.4 (National Institute of Health) and normalized to reference samples after obtaining multiple exposures to ensure linearity of data capture. To allow for direct comparisons within each sample set, protein lysates from each gender and each brain region were electrophoresed, transferred, immunoblotted and exposed simultaneously.

Synaptosomal [^{3}H]-5-HT transport activity measurements

Mouse brain synaptosomes were prepared as previously described (Zhu *et al.* 2011). Briefly, freshly dissected brain tissues were homogenized in 0.32 M sucrose buffer with 10 mM HEPES and 2 mM EDTA (pH 7). P2 pellets were obtained by centrifugation, resuspended in Krebs-Ringer-HEPES (KRH) assay buffer containing 130 mM NaCl, 1.3 mM KCl, 2.2 mM $CaCl_2$, 1.2 mM $MgSO_4$, 1.2 mM KH_2PO_4, 1.8 g/l D-glucose, 10 mM HEPES, pH 7.4, 100 μM pargyline and 100 μM ascorbic acid and protein was quantified by BCA method (Pierce). Radiolabeled [^{3}H]-5-HT (20 nM) uptake into synaptosomes (40 μg) was performed for 10 min at 37°C and terminated using a Brandel Cell Harvester (Brandel, Gaithersburg, MD, USA), as previously described. Non-specific uptake was determined using parallel samples

incubating with 10 μM paroxetine with levels here subtracted from total accumulation to yield specific uptake activity.

RNA isolation and qPCR

Total RNA was extracted from individual brain regions of age-matched C57BL/6J and DBA/2J mouse pairs using RNeasy Midi Kit (Qiagen, Venlo, The Netherlands) following the manufacturer's instructions. RNA concentrations were determined by NanoDrop ND-1000 (NanoDrop Technologies, Wilmington, DE, USA). Reverse transcription reactions were carried out using SuperScript III First-Strand Synthesis Kit (Invitrogen, Life Technologies, Grand Island, NY, USA). Briefly, 1 μg of total RNA was used as template to synthesize first-strand complementary DNA using oligo(dT)$_{20}$ primer. A 926-bp *Pcdh15* complementary DNA (cDNA) fragment covering exons 1 through 6 was amplified by PCR using the following oligonucleotides: 5′ -AGATAGAGGGCCTGCGGATG-3′ (RB4499) and 5′ -TAGCTCCATTGTCTCCCGAGAAC-3′ (RB4502). As a control, a 152-bp *Gapdh* cDNA fragment was also amplified from the same samples using the following primer set: 5′ -GCACAGTCAAGGCCGAGAAT-3′ (RB4495) and 5′ -GGCCTTCTCCATGGTGGTGAA-3′ (RB4496). Quantitative PCR (qPCR) was performed using KAPA SYBR FAST Universal qPCR Kit (Kapa Biosystems, Wilmington, MA, USA) on an Eco PCR system (Illumina, San Diego, CA, USA). The PCR products were amplified from cDNAs and each reaction was carried out in triplicate. The polymerase activation step at 95°C for 10 min was followed by 40 cycles of 15 seconds at 95°C and 60 seconds at 60°C. The $2^{-\Delta Ct}$ method was used to analyze the relative changes of gene expression using GAPDH as reference (Schmittgen & Livak 2008). Oligonucleotides used for *Pcdh15* qPCR were 5′ -CATGAAGTAC GCATCGTGGT-3′ (RB4563) and 5′ -TAGCTCCATTGTCTCCCGAGAAC-3′ (RB4502) to yield a 121-bp PCR product.

Midbrain transcriptome profiling

Midbrain microarray analyses on the BXD strains were performed as previously described (Ye *et al.* 2014). Briefly, an Agilent-028005 SurePrint G3 Mouse GE 8x60K platform was used for mRNA probe hybridization. Raw expression data were then normalized and rescaled followed by an internal validation using sample-specific genetic markers. The final verified data have been deposited in GEO and in GN and reflects this systematic genotype QC process (accession number GN381).

Data analyses

Data were analyzed using standard analysis of variance (ANOVA) and correlation analysis using Stata 11 (Stata Corp, College Station, TX, USA) and Prism 5 (GraphPad, Software Inc, La Jolla, CA, USA). Quantitative trait locus mapping was performed using the WebQTL module of the GeneNetwork (http://www.genenetwork.org). Adjusted heritability (h^2) of the traits was estimated using Hegmann and Possidente's method (Hegmann & Possidente 1981). Significance of heritability was calculated by the *F* -test comparing within-strain vs. between-strain variances. Quantitative trait loci were calculated from the likelihood ratio statistic (LRS) and logarithm of odds (LOD) scores. Statistical significance was determined using 2000 permutations. Significant QTLs were defined as the LRS value

that represents a genome-wide *P* value of 0.05. Suggestive QTLs were defined as having an LRS value a genome-wide *P* value of 0.63 (Lander & Kruglyak 1995). Confidence intervals were determined as the location at which the LOD value is reduced by 1.5. A 1.5 LOD cutoff has been estimated to reflect a 95% confidence that genes driving the QTL lie within this range (Dupuis & Siegmund 1999; Visscher *et al.* 1996). Phenotypic correlation analyses were performed by comparing measured 5-HT traits with archived BXD phenotypes in the GeneNetwork database, with correlation coefficients and *P* values calculated using Spearman's rank tests (uncorrected $P < 0.05$ was considered significant). Transcriptome-derived gene networks were generated by Cytoscape 2.8.3 (Cytoscape Consortium, San Diego, CA, USA) using input data files (node and network) from WebQTL correlation analysis module.

Online data access

SERT protein expression levels for the BXD strains determined in this study have been deposited in the GeneNetwork database at http://www.genenetwork.org under the category of Central Nervous System: Protein Expression.

Results

Midbrain SERT mRNA expression and associated gene networks

Previously (Ye *et al.* 2014), we described our transcriptome profiling of adult male midbrain mRNAs across BXD strains using microarray analyses. When we inspected the variation of SERT mRNA levels across these same lines, we found that expression levels were not significantly heritable ($P = 0.49$, $h^2 = 0.16$). On the basis of this observation, we did not pursue expression QTL (eQTL) analysis on the SERT mRNA data. Non-genetic factors, including individual animal variation and the potential impact of environmental factors, can diminish power in heritability estimates. However, correlational analysis within the same dataset does not rely solely on the genetic control of between-strain variations. Therefore, we turned to an intracorrelation analysis of mRNAs within the male midbrain transcriptome using strain means. We extracted genes whose expression significantly correlated positively (1511 genes) or negatively (1126 genes) with *Slc6a4* mRNA levels across BXD lines (uncorrected $P < 0.05$, Table S2). In Fig. 1a we present the top 25 correlated genes in a network diagram to highlight the strong intracorrelations among these genes. The composition of this network suggests that it reflects a realistic delineation of genes whose expression is associated with *Slc6a4* gene expression. For example, the strongest correlations were found for *Fev*, *Tph2*, *Gch1* and *Slc18a2*. *Fev* is a transcription factor (also known as PET-1) and master regulator of CNS 5-HT neuron identity, expressed at the beginning of raphe neuron commitment to a serotonergic identity (Hendricks *et al.* 2003). *Tph2* encodes the rate-limiting enzyme in 5-HT biosynthesis, whereas *Gch1* encodes the rate-limiting enzyme in the synthesis of tetrahydrobiopterin, an essential cofactor for amino acid decarboxylase that converts 5-hydroxytryptophan to 5-HT. *Slc18a2* encodes VMAT2, the transporter responsible for packaging 5-HT into synaptic vesicles prior to release.

To specify further the possible contributions of *Slc6a4*-associated transcripts to 5-HT biosynthesis we used *Tph2* gene expression as a seed for a second network analysis. Here,

we found 1209 genes with significant positive correlations with *Tph2* gene expression and 1287 with negative correlations (Fig. 1b and Table S2). When we compared the *Slc6a4*- and *Tph2*-seeded gene lists, significant overlap was found. In fact, more than a third of the top 100 correlated genes correlated with *Slc6a4* and Tph2 were common (Fig. 1c and Table S2). As expected, *Fev* , *Gch1*, *Ddc* and *Slc18a2* were among the 22 genes in this group with significant *positive* correlations. Additionally, we identified several genes that had not been previously implicated in serotonergic signaling, including the Na^+/bile acid co-transporter (*Slc10a4*) and the synaptic cell adhesion molecule (CAM) neuroligin 2 (*Nlgn2*). In this analysis, we also identified 16 genes whose expression was *negatively* correlated with the expression of both *Slc6a4* and *Tph2*. To our knowledge, none of these genes, including interleukin 2 (*Il2*), cortexin 3 (*Ctxn3*) and the restless leg syndrome (RLS) risk gene *Btbd9*, have been identified as correlates of 5-HT signaling. Finally, in Table S2, we note genes whose expression is associated positively or negatively with the expression of *Slc6a4* but not of *Tph2*. The latter data may point to pathways of *Slc6a4* gene regulation that provide constitutive support of SERT biosynthesis and trafficking or that exert non-cell autonomous regulation of 5-HT inactivation.

Conceivably, the midbrain gene expression networks we identified could be of more general relevance to neuronal function in the midbrain, rather than specific determinants of serotonergic signaling. To examine this issue, we extracted gene expression clusters likely to be more related to dopamine (DA) homeostasis by using as seeds the genes encoding tyrosine hydroxylase (*Th*) and the DA transporter (*Slc6a3*). We also generated an acetylcholine (ACh)-linked gene expression network by using as seeds the genes encoding choline acetyltransferase (*Chat*) and the presynaptic choline transporter (*Slc5a7*) (Tables S3,S4 and Figs. S1,S2). Only genes that encode shared determinants of monoaminergic biosynthesis and packaging, such as *Ddc* and *Slc18a2*, were identified as genes contributing to more than one network. These findings indicate that the networks seeded by *Slc6a4* gene mRNA profiles are specifically tuned to *Slc6a4* transcription.

Variation and heritability of BXD SERT protein levels

It is well known that protein levels do not always highly correlate with levels of mRNA, particularly when the protein is subject to extensive post-translational regulation, as is the case for SERT (Steiner *et al.* 2008). To gain additional insights into networks associated with SERT protein expression, we used immunoblotting techniques to quantify SERT protein levels in the midbrain and diencephalon of 38 BXD RI strains. We found that SERT protein expression varied significantly across BXD strains in both brain regions (Fig. 2). BXD strain variation contributed significantly to the overall variation in SERT protein expression in the midbrain of both genders, indicating high heritability (males: $F_{33,30} = 6.78$, $P < 0.0001$, $h^2 = 0.77$; females: $F_{28,26} = 10.85$, $P < 0.0001$, $h^2 = 0.84$). A similar pattern was detected for diencephalon SERT protein levels for females ($F_{28,27} = 2.75$, $P = 0.005$, $h^2 = 0.58$). In contrast, analysis of male diencephalon SERT protein expression yielded no evidence of heritability ($F_{33,31} = 1.34$, $P = 0.21$, $h^2 = 0.40$), likely owing to the higher variation among animals from the same strain. However, SERT midbrain and diencephalon protein expression levels did not correlate for either gender (males: $r = 0.02$, $P = 0.90$; females: $r = 0.11$, $P = 0.58$), consistent with region-specific factors contributing to trait

variation. Finally, SERT protein levels did not correlate between genders in either region (midbrain: $r = 0.02$, $P = 0.90$; diencephalon: $r = 0.27$, $P = 0.20$).

Phenotypic correlates of SERT protein expression

The quantification of SERT protein levels from the same animals for which 5-HT measures were acquired (Ye *et al.* 2014) provided an opportunity to examine whether the two indices correlate with each other across strains. In midbrain, SERT protein levels in males positively correlated with 5-HT levels ($r = 0.40$, $P = 0.02$), but not with 5-HIAA ($r = 0.25$, $P = 0.15$) or 5-HT turnover rates ($r = -0.23$, $P = 0.19$). Interestingly, this correlation was not evident in females (5-HT: $r = 0.18$, NS; 5-HIAA: $r = 0.13$, NS; 5-HT turnover: $r = -0.02$, NS). Although the correlations between male diencephalon SERT levels and 5-HT levels or 5-HT turnover rates fell short of statistical significance (5-HT: $r = 0.32$, $P = 0.09$; 5-HT turnover: $r = 0.27$, $P = 0.16$), we did observe a significant, positive correlation between female SERT levels and 5-HIAA levels ($r = 0.54$, $P = 0.002$). Next, we extracted phenotypes from the GeneNetwork collection that demonstrate significant association with SERT levels (Table S5). Consistent with the behavioral changes associated with 5-HT manipulations, we found a number of anxiety measures that correlated with both midbrain and diencephalon SERT levels, regardless of gender. Interestingly, multiple cocaine response traits, including conditioned place preference tests and locomotor sensitization, were significantly correlated with female, but not male diencephalon SERT levels, whereas these measures lacked association with midbrain SERT levels regardless of gender.

QTLs associated with BXD SERT protein expression

Through assessment of DNA polymorphisms that associate with variation in SERT protein levels, we identified putative QTLs and inspected gene lists that may dictate SERT protein variation across BXD lines (Table S6). In Fig. 3, we present plots of these QTLs divided by brain region and gender. None of the QTLs noted below encompass the region containing the *Slc6a4* gene on chromosome 11, suggesting a limited influence of *Slc6a4* gene variation on steady-state SERT protein levels. As expected from the absence of intercorrelations by region or gender of BXD SERT variation, the same QTLs were not evident between midbrain and diencephalon, regardless of gender. With respect to male midbrain SERT levels, we identified one significant and three suggestive QTLs (Fig. 3a): *mbsertq1* on chromosome 3 (30 Mb, LOD = 2.93), *mbsertq2* on chromosome 7 (140 Mb, LOD = 2.26), *mbsertq3* on chromosome 10 (73 Mb, LOD = 2.25) and significant QTL *mbsertq4* on chromosome 19 (59.5 Mb, LOD = 3.58). It is worth noting that *mbsertq3* was also identified as a suggestive QTL for midbrain 5-HT levels in our previous report (Ye *et al.* 2014).

From the mapping of female midbrain SERT levels (Fig. 3b), we found a suggestive QTL (*mbsertq5*) on chromosome 8 (91 Mb, LOD = 2.68). In female diencephalon (Fig. 3d), there is a suggestive QTL (*dcsertq1*) on chromosome 13 (108 Mb, LOD = 3.09) and another suggestive QTL (*dcsertq2*) on chromosome 18 (69.5 Mb, LOD = 2.59). Because we did not detect significant strain effects for male diencephalon SERT levels, as expected, we did not find QTL peaks above suggestive threshold for these samples (Fig. 3c).

A male midbrain transcriptome linked to SERT protein expression

Although multiple determinants of *Slc6a4* mRNA expression in the BXD lines were identified in our network analysis above, these genes need not be the major drivers for the variation in SERT protein levels we detected across strains. Indeed, when we compared midbrain SERT protein levels and *Slc6a4* mRNA across the same lines, the two traits did not exhibit a significant correlation ($r = -0.36$, $P = 0.18$). These findings suggest that significant post-transcriptional regulation is imposed to dictate the SERT protein variation we observed across BXD lines. In Fig. 4a we plot the 25 genes whose expression profiles correlated strongly, negatively or positively, with male midbrain SERT protein levels across BXD lines. The entire list of correlated mRNAs is found in Table S7. When we compared these transcripts with the genes encompassed by the QTLs nominated above, 42 genes were present on both lists (Fig. 4b and Table S8). We compared these genes with a similar collection of genes whose expression correlated with 5-HT levels and also could be found within a 5-HT QTL (Suppl File 10 in Ye *et al.* 2014). This analysis yielded a single gene, *Pcdh15*.

Pcdh15 as a determinant of SERT protein expression and 5-HT homeostasis

As indicated above, *Pcdh15* lies within suggestive QTLs for both male midbrain SERT protein levels (*mbsertq3*) and midbrain (pooled gender) 5-HT levels (*mb5htq3*) on chromosome 10. Moreover, marker regression analyses revealed that for both traits, the same single nucleotide polymorphism (SNP, rs13480650), located in the intron between exons 1 and 2 of *Pcdh15*, exhibited highest association (Fig. 5a). Adding strength to the possibility that variation in *Pcdh15* could influence both SERT and 5-HT levels, strain means of BXD lines segregated by rs13480650 variation revealed that 5-HT, 5-HT turnover, SERT mRNA and protein levels exhibited significant differences (Fig. 5b–e).

The principle phenotype associated with *Pcdh15* loss of function is a perturbation of hair cell mechanosensitivity, with resulting alterations in vestibular reflexes (Ahmed *et al.* 2001; Alagramam *et al.* 2001; Xiong *et al.* 2012). Although the most visible signs of *Pcdh15* function relate to vestibular function, our finding of associations of a *Pcdh15* SNP with multiple serotonergic traits suggests a more widespread expression, and influence, of the gene. Indeed, using RT-PCR on mRNA isolated from adult male C57BL/6J and DBA/2J mice, we readily detected *Pcdh15* expression in midbrain, cerebellum, hippocampus, striatum and frontal cortex (Fig. 6a). As amplifications of midbrain extracts from C57BL/6J mice consistently displayed higher levels of *Pcdh15* than DBA/2J extracts, we pursued further quantitative analyses. Consistent with semiquantitative estimates, qPCR analysis of midbrain *Pcdh15* gene expression (Fig. 6b) revealed significantly higher levels of *Pcdh15* mRNA in midbrain samples of C57BL/6J vs. DBA/2J mice ($P < 0.05$).

Evaluation of SERT and 5-HT in Pcdh15$^{av\text{-}3J}$ mice

To provide a direct test of whether changes in *Pcdh15* expression impact 5-HT homeostasis, we measured 5-HT and 5-HIAA levels in *Pcdh15*$^{av\text{-}3J}$ mice (on C57BL/6J background) that generate a truncated, functional null PCDH15 protein owing to the introduction of a premature stop codon in exon 12 (Alagramam *et al.* 2001). This mutation leads to cochlear hair cell abnormalities and a distinct circling phenotype (Alagramam *et al.* 2001). We found

that midbrain 5-HT levels of *Pcdh15*$^{av\text{-}3J}$ homozygous mice were significantly higher than those measured in WT littermate samples ($P < 0.005$, Fig. 7a). Interestingly, this increase was not evident in hippocampal extracts (data not shown). For this analysis, we chose to use both genders to maintain consistency with the 5-HT trait used to identify the QTL. We did not detect gender differences in 5-HT levels within the same *Pcdh15* genotype group. Additionally, the same relationship between 5-HT levels and *Pcdh15* gene dosage was observed in both genders with a stronger effect in males, likely a result of larger sample sizes in the male group (Fig. S3). Levels of 5-HIAA did not exhibit genotype effects in any brain region. However, hippocampus, striatal and midbrain samples of *Pcdh15*$^{av\text{-}3J}$ homozygous mice demonstrated significantly lower 5-HIAA/5-HT turnover ratios than their WT littermates ($P < 0.05$, Fig. 7b–d). To assess whether these changes are specific to 5-HT traits, we measured DA, the DA metabolite dihydroxyphenylalanine (DOPAC) and estimated DA turnover (DOPAC/DA) in these same samples and found no genotype difference in any brain region (data not shown).

Next, we asked whether *Pcdh15*$^{av\text{-}3J}$ mice exhibit changes in male SERT protein levels. Immunoblotting studies (Fig. 8a) revealed significantly increased SERT levels in both the midbrain and striatum of *Pcdh15*$^{av\text{-}3J}$ homozygous mice relative to WT littermates (midbrain: $P < 0.01$; striatum: $P < 0.05$). *Pcdh15*$^{av\text{-}3J}$ homozygous mice also displayed a trend to lower striatal DA transporter (DAT) levels, though this difference did not reach statistical significance ($P = 0.06$) (Fig. 8b).

To examine whether the increased SERT protein levels observed in *Pcdh15*$^{av\text{-}3J}$ homozygous mice translates into higher levels of 5-HT uptake, we prepared male midbrain and hippocampal synaptosomes and quantified paroxetine-sensitive 5-HT uptake in these preparations, as described in *Materials and methods* (Fig. 9). Consistent with the changes in SERT protein levels, these studies demonstrated significant increases in the rates of synaptosomal 5-HT uptake in the *Pcdh15*$^{av\text{-}3J}$ homozygous mice for both mid-brain and hippocampus (midbrain: $P < 0.001$; hippocampus: $P < 0.05$) vs. littermate WT animals.

Discussion

SERT plays a critical role in limiting synaptic 5-HT availability and is the principal target for the most highly prescribed medications used to treat depression. Animal models with genetic manipulations of SERT expression (Murphy & Lesch 2008; Veenstra-VanderWeele *et al.* 2012) and human studies on functional SERT gene variation (Caspi *et al.* 2003; Veenstra-VanderWeele *et al.* 2012) support the hypothesis that perturbed SERT function or regulation can modify behavior and increase the risk for multiple neuropsychiatric disorders. Here, we capitalized on the availability of the BXD reference panel to search for molecular determinants and phenotypic correlates of SERT mRNA and protein expression.

One opportunity afforded by the assessment of trait variation across BXD lines (e.g. *Slc6a4* mRNA levels and SERT protein levels) is the ability to map putative QTLs that lead to the identification of genes that control trait expression. As we were unable to document heritability of *Slc6a4* mRNA variation, an eQTL analysis was inappropriate. However, correlational analyses within the same mRNA dataset make use of the rank order of strains,

a variable that adds dimensionality to an evaluation otherwise dependent on trait mean differences. Moreover, by calculating intercorrelations between gene expression profiles we were not limited by the genetic control of gene expression, instead asking questions on the co-varying expression pattern of genes regardless of the upstream determinants. In this context, we first sought to identify genes whose mRNA expression significantly correlates with that of *Slc6a4*. Using a previously generated male midbrain transcriptome (Ye *et al.* 2014), and bioinformatics methods to relate correlated genes to another, we generated networks of genes that both positively and negatively correlated with *Slc6a4* expression. In this effort, we identified the expression of *Fev* , *Tph2*, *Gch1*, *Ddc* and *Slc18a2* as positively related to *Slc6a4* expression. These finding were reassuring, as *Fev* is known to be an essential determinant of 5-HT neuron identity, which includes the expression of genes needed to synthesize and package 5-HT (Deneris 2011). Moreover, we found little overlap in the *Slc6a4* network with networks generated using determinants of dopaminergic and cholinergic identity, including networks linked to other presynaptic transporters.

To classify genes in the *Slc6a4* network that may associate with the transporter's expression based on common effects on multiple aspects of 5-HT neuron identity, vs. more specifically on *Slc6a4*, we first evaluated genes in the *Slc6a4* network for their association with a *Tph2*-seeded network. *Positively correlated genes*: Besides the genes in the 5-HT biosynthetic and release pathway noted above, we also identified, among others (Table S2), *Slc10a4* and *Nlgn2*. Consistent with our serotonergic network analyses, inspection of the adult mouse CNS expression pattern *Slc10a4*, which encodes an orphan Na /bile acid co-transporter, reveals significant enrichment in+the dorsal and median raphe nuclei (Hawrylycz *et al.* 2011). Evidence has also been advanced that *Slc10a4* is involved in dopaminergic and cholinergic signaling, mainly based on its co-localization with the vesicular transporters VAChT and VMAT2 (Borges 2013; Burger *et al.* 2011). Our findings concur with these observations, as we also found *Slc10a4* among the cholinergic and dopaminergic gene-seeded networks. These findings indicate that the activity of *Slc10a4* likely contributes to common features of monoaminergic neurotransmission, such as the packaging of cationic neurotransmitters. *Nlgn2* encodes neuroligin2 (NLGN2), a cell adhesion protein. NLGNs have been characterized as postsynaptic binding partners of presynaptic neurexin proteins, and are thought to mediate synaptogenesis and synapse identity (Sudhof 2008; Varoqueaux *et al.* 2006). NLGN2 has been shown to be co-localized and associated with $GABA_A$ receptors, as well as with the postsynaptic scaffolding proteins gephyrin and collybistin (Poulopoulos *et al.* 2009). The SNPs and copy number variations of *NLGN2* have been implicated in schizophrenia (Sun *et al.* 2011) and mental retardation (Belligni *et al.* 2012). Further studies are needed to explore the potential role of NLGN2 in 5-HT signaling, though one possibility is that the protein plays a role in GABAergic inhibition of raphe neurons (Bagdy *et al.* 2000; Soiza-Reilly *et al.* 2013). *Negatively correlated genes*: One gene of note in this group is *Btbd9*, a gene named for the presence of a BTB protein–protein association domain (Perez-Torrado *et al.* 2006), but whose cellular function is unclear, though it has been associated in human genetic studies with RLS (DeAndrade *et al.* 2012). Because reduced CSF 5-HIAA levels have been reported in RLS subjects (Earley *et al.* 2001), RLS has been reported to be a side effect of SSRI administration (Rottach *et al.* 2008), and

BTBD9 KO mice display alterations in striatal 5-HIAA levels (DeAndrade *et al.* 2012); further study of Btb9/RLS/5-HT connections should be pursued.

Because mRNA levels do not always correlate with protein expression levels and SERT undergoes extensive post-transcriptional regulation (Ramamoorthy *et al.* 2011; Steiner *et al.* 2008), we evaluated BXD strain variation of SERT protein levels using quantitative Western blotting methods. In contrast to our inability to document significant heritability with the strain variation in *Slc6a4* mRNA expression, SERT protein expression demonstrated significant heritability. Our studies show that midbrain and diencephalon SERT levels are under the control of distinct, heritable factors, as might be expected given the distinct needs of these regions to modulate 5-HT signaling. Even within regions, gender-specific influences are evident, as male and female variation in SERT levels did not correlate across strains. In recognition of these issues, we assessed phenotypic traits and QTLs for each region and gender separately. It is important to note that although determinants of strain variation in SERT levels or the transporter's relationship with phenotypes were found to be region and gender specific, we must realize that (1) the availability of animals per BXD strain in this study limited the statistical power to uncover some of the relationships, and (2) such relationships may change, or be more evident under other conditions. For example, a major determinant of midbrain SERT protein levels in response to stress could be shared by males and females, but differ in their relative impact under non-stressful conditions.

The dense mapping of SNPs across the genomes of the parental strains of the BXD lines affords an opportunity to search for genes where genetic variation may drive SERT protein expression. In this regard, we identified one significant and six suggestive SERT protein level QTLs. Because of the number and local density of markers involved in these analyses, and disequilibrium that likely exists among neighboring genes, these QTLs, and the genes that lie within them (1.5 LOD from the peak), can only serve as hypothesis generators that should be confirmed through independent approaches. With respect to the significant QTL *mbsertq4*, a plausible candidate gene within this QTL is *Slc18a2*, which encodes VMAT2. BXD lines bearing the *D* variants of the closest SNP to *Slc18a2* (rs6191324) have higher SERT expression levels than strains bearing the *B* variants (Fig. S4a). The strains bearing the *D* variant also show higher VMAT2 mRNA levels (Fig. S4b). One hypothesis, therefore, that could link *Slc18a2* gene variation to SERT protein levels and *Slc18a2* mRNA expression is that the level of VMAT2, known to determine the quantity of 5-HT stored in synaptic vesicles (Fon *et al.* 1997), drives a positive-feedback, autoregulatory process that in turn ensures that as more 5-HT is packaged and released, more SERT protein is available to clear released 5-HT. Consistent with this idea, male midbrain 5-HT levels positively correlated with midbrain SERT protein levels, and variation in rs6191324 associates with both midbrain and blood 5-HT (Fig. S4c,d). We must recognize that rs6191324 has an unknown functional relationship to VMAT2, as it does not alter VMAT2 coding sequences or any known *Slc18a2* regulatory sequences. However, DBA/2J mice and C57BL/6J mice differ by two amino acids, L117/S505 vs. P117/P505, respectively, and this variation associates with SSRI-sensitive behaviors (Crowley *et al.* 2006).

Given the suggestive nature of the other SERT protein QTLs, we refrain from further discussion of candidate genes responsible for these associations, except for *mbsertq3*. This

QTL is striking to us as it also appeared in our previous analysis of midbrain 5-HT variation (Ye *et al.* 2014). Moreover, *Pcdh15* mRNA expression was also found to correlate with SERT protein expression. *Pcdh15* belongs to the family of non-clustered protocadherins in the protocadherin superfamily (Kim *et al.* 2011; Morishita & Yagi 2007). Protocadherins are a subset of CAMs that mediate the formation, maturation and specification of synapses. Different brain regions express distinct combinations of synaptic CAMs (O'Rourke *et al.* 2012). With respect to our study, a protocadherin gene family, *Pcdha*, was demonstrated to have important functions in controlling 5-HT axonal fiber density in multiple brain regions (Katori *et al.* 2009). Over the last decade, the synaptic CAMs have been implicated in multiple neuropsychiatric diseases, such as autism and schizophrenia (for reviews, see Hortsch & Umemori 2009; Ye *et al.* 2010). The human locus 10q21.1, where *PCDH15* is located, has been associated with Crohn's disease (Rioux *et al.* 2007) and late-onset Alzheimer's disease (Myers *et al.* 2000). Recently, a 386-kb deletion on 10q21.1, including the first three exons of *PCDH15*, was reported in a subject with autism spectrum disorder (Sorte *et al.* 2013). Although primarily recognized as a disease associated with deafness and blindness, more than 20% of Usher syndrome patients display psychiatric symptoms (Carvill 2001) and comorbidities of Usher syndrome with various mental illnesses are well documented (Domanico *et al.* 2012; Rao *et al.* 2010; Rijavec & Grubic 2009). Our findings suggest that there may be genetic components that underlie these symptoms and that relate to perturb 5-HT signaling, though further studies are needed to assess possible relationships.

To test whether *Pcdh15* gene expression dictates SERT protein levels, as well as 5-HT traits, we first confirmed that midbrain *Pcdh15* gene expression varies between C57BL/6J and DBA/2J strains using qPCR approaches. Indeed, we found that levels of *Pcdh15* mRNA in C57BL/6J mice were significantly higher than those measured in DBA/2J mice. Additionally, we found that lines bearing C57BL/6J alleles of *Pcdh15* exhibit both lower SERT protein expression and lower 5-HT levels (Fig. 5), suggesting a negative regulation of SERT and 5-HT homeostasis by the cell adhesion protein.

To move beyond correlation studies, we pursued a characterization of mice bearing a functional null mutation in *Pcdh15* (*Pcdh15*$^{av\text{-}3J}$) (Alagramam *et al.* 2001). In support of our hypothesis that *Pcdh15* expression negatively regulates both SERT protein levels and 5-HT traits, we found that homozygous *Pcdh15*$^{av\text{-}3J}$ mice exhibited an increase (~75%) in midbrain SERT protein expression. A significant increase was also evident in striatum, whereas DAT levels in this region were unchanged. We also observed an increase (~30%) in midbrain 5-HT levels when compared with WT littermates. To determine if SERT expression has a reciprocal impact on *Pcdh15* expression, we also compared midbrain *Pcdh15* gene expression levels between WT and SERT KO mice (both on C57BL/6J background). We did not detect a significance difference in this measure (SERT KO/WT = 1.14 ± 0.19, $N = 3$ for each genotype).

The studies with *Pcdh15*$^{av\text{-}3J}$ raise the obvious question as to how PCDH15 protein modulates serotonergic phenotypes. Unfortunately, the currently available antibodies proved insufficiently specific to document the cellular localization of PCDH15 protein. Therefore, we returned to an assessment of mRNA expression patterns linked to *Pcdh15* mRNA in the midbrain. *Pcdh15* is a large gene (>400 kb, with >30 exons) and its transcripts exhibit at

least 14 distinct splicing variants. As we cannot at present select microarray probes based on spliced products linked to 5-HT signaling, we chose a broader strategy to define a network of *Pcdh15* mRNA-associated genes, using a probe (A_55_P2176176) that hybridizes with 12 *Pcdh15* splicing isoforms (Fig. S5a). We then extracted those genes that demonstrated highest correlations with SERT protein expression. This effort yielded 330 such genes (Table S9). The list was reduced to 31 genes when we raised the correlation *P* value to 0.01 (Fig. S5b, Table S9). Among this list we note *Syngr4*, a tetraspanin protein among a class of proteins that associate with synaptic vesicles (Belizaire *et al.* 2004; Stevens *et al.* 2012). A closely related protein, synaptogyrin 3, has been found to associate with DAT (Egana *et al.* 2009). We speculate that synaptogyrin 4 may associate with SERT or with synaptic vesicles that secrete 5-HT. Clearly, further studies that assess the impact of the $Pcdh15^{av\text{-}3J}$ mutation on 5-HT neuron development and function are needed, possibly through the use of conditional deletion strategies. In summary, our studies nominate a network of genes that regulate, or are regulated by *Slc6a4* expression and/or SERT protein levels. Because of its common association with transporter and 5-HT levels, our studies reveal that one of these genes, *Pcdh15*, plays an unappreciated role in 5-HT signaling, and thus may contribute to multiple neuropsychiatric disorders.

Supplementary Material

Refer to Web version on PubMed Central for supplementary material.

References

Ahmed ZM, Riazuddin S, Bernstein SL, Ahmed Z, Khan S, Griffith AJ, Morell RJ, Friedman TB, Wilcox ER. Mutations of the protocadherin gene PCDH15 cause Usher syndrome type 1F. Am J Hum Genet. 2001; 69:25–34. [PubMed: 11398101]

Alagramam KN, Murcia CL, Kwon HY, Pawlowski KS, Wright CG, Woychik RP. The mouse Ames waltzer hearing-loss mutant is caused by mutation of Pcdh15, a novel protocadherin gene. Nat Genet. 2001; 27:99–102. [PubMed: 11138007]

Andreux PA, Williams EG, Koutnikova H, Houtkooper RH, Champy MF, Henry H, Schoonjans K, Williams RW, Auwerx J. Systems genetics of metabolism: the use of the BXD murine reference panel for multiscalar integration of traits. Cell. 2012; 150:1287–1299. [PubMed: 22939713]

Azmitia EC. Serotonin and brain: evolution, neuroplasticity, and homeostasis. Int Rev Neurobiol. 2007; 77:31–56. [PubMed: 17178471]

Bagdy E, Kiraly I, Harsing LG Jr. Reciprocal innervation between serotonergic and GABAergic neurons in raphe nuclei of the rat. Neurochem Res. 2000; 25:1465–1473. [PubMed: 11071365]

Belizaire R, Komanduri C, Wooten K, Chen M, Thaller C, Janz R. Characterization of synaptogyrin 3 as a new synaptic vesicle protein. J Comp Neurol. 2004; 470:266–281. [PubMed: 14755516]

Belligni EF, Di Gregorio E, Biamino E, Calcia A, Molinatto C, Talarico F, Ferrero GB, Brusco A, Silengo MC. 790 Kb microduplication in chromosome band 17p13.1 associated with intellectual disability, afebrile seizures, dysmorphic features, diabetes, and hypothyroidism. Eur J Med Genet. 2012; 55:222–224. [PubMed: 22365944]

Berger M, Gray JA, Roth BL. The expanded biology of serotonin. Annu Rev Med. 2009; 60:355–366. [PubMed: 19630576]

Blakely RD, Berson HE, Fremeau RT Jr. Caron MG, Peek MM, Prince HK, Bradley CC. Cloning and expression of a functional serotonin transporter from rat brain. Nature. 1991; 354:66–70. [PubMed: 1944572]

Borges K. Slc10A4 – what do we know about the function of this “secret ligand carrier” protein? Exp Neurol. 2013; 248C:258–261. [PubMed: 23810836]

Burger S, Doring B, Hardt M, Beuerlein K, Gerstberger R, Geyer J. Co-expression studies of the orphan carrier protein Slc10a4 and the vesicular carriers VAChT and VMAT2 in the rat central and peripheral nervous system. Neuroscience. 2011; 193:109–121. [PubMed: 21742018]

Carneiro AM, Airey DC, Thompson B, Zhu CB, Lu L, Chesler EJ, Erikson KM, Blakely RD. Functional coding variation in recombinant inbred mouse lines reveals multiple serotonin transporter-associated phenotypes. Proc Natl Acad Sci U S A. 2009; 106:2047–2052. [PubMed: 19179283]

Carvill S. Sensory impairments, intellectual disability and psychiatry. J Intellect Disabil Res. 2001; 45:467–483. [PubMed: 11737534]

Caspi A, Sugden K, Moffitt TE, Taylor A, Craig IW, Harrington H, McClay J, Mill J, Martin J, Braithwaite A, Poulton R. Influence of life stress on depression: moderation by a polymorphism in the 5-HTT gene. Science. 2003; 301:386–389. [PubMed: 12869766]

Crowley JJ, Brodkin ES, Blendy JA, Berrettini WH, Lucki I. Pharmacogenomic evaluation of the antidepressant citalopram in the mouse tail suspension test. Neuropsychopharmacology. 2006; 31:2433–2442. [PubMed: 16554742]

DeAndrade MP, Johnson RL Jr. Unger EL, Zhang L, van Groen T, Gamble KL, Li Y. Motor restlessness, sleep disturbances, thermal sensory alterations and elevated serum iron levels in Btbd9 mutant mice. Hum Mol Genet. 2012; 21:3984–3992. [PubMed: 22678064]

Deneris ES. Molecular genetics of mouse serotonin neurons across the lifespan. Neuroscience. 2011; 197:17–27. [PubMed: 21920412]

Domanico D, Fragiotta S, Trabucco P, Nebbioso M, Vingolo EM. Genetic analysis for two Italian siblings with usher syndrome and schizophrenia. Case Rep Ophthalmol Med. 2012; 2012:380863. [PubMed: 23091761]

Dupuis J, Siegmund D. Statistical methods for mapping quantitative trait loci from a dense set of markers. Genetics. 1999; 151:373–386. [PubMed: 9872974]

Earley CJ, Hyland K, Allen RP. CSF dopamine, serotonin, and biopterin metabolites in patients with restless legs syndrome. Mov Disord. 2001; 16:144–149. [PubMed: 11215576]

Egana LA, Cuevas RA, Baust TB, Parra LA, Leak RK, Hochendoner S, Pena K, Quiroz M, Hong WC, Dorostkar MM, Janz R, Sitte HH, Torres GE. Physical and functional interaction between the dopamine transporter and the synaptic vesicle protein synaptogyrin-3. J Neurosci. 2009; 29:4592–4604. [PubMed: 19357284]

Fon EA, Pothos EN, Sun BC, Killeen N, Sulzer D, Edwards RH. Vesicular transport regulates monoamine storage and release but is not essential for amphetamine action. Neuron. 1997; 19:1271–1283. [PubMed: 9427250]

Hawrylycz M, Ng L, Page D, Morris J, Lau C, Faber S, Faber V, Sunkin S, Menon V, Lein E, Jones A. Multi-scale correlation structure of gene expression in the brain. Neural Netw. 2011; 24:933–942. [PubMed: 21764550]

Hegmann JP, Possidente B. Estimating genetic correlations from inbred strains. Behav Genet. 1981; 11:103–114. [PubMed: 7271677]

Hendricks TJ, Fyodorov DV, Wegman LJ, Lelutiu NB, Pehek EA, Yamamoto B, Silver J, Weeber EJ, Sweatt JD, Deneris ES. Pet-1 ETS gene plays a critical role in 5-HT neuron development and is required for normal anxiety-like and aggressive behavior. Neuron. 2003; 37:233–247. [PubMed: 12546819]

Hoffman BJ, Mezey E, Brownstein MJ. Cloning of a serotonin transporter affected by antidepressants. Science. 1991; 254:579–580. [PubMed: 1948036]

Homberg JR, Lesch KP. Looking on the bright side of serotonin transporter gene variation. Biol Psychiatry. 2011; 69:513–519. [PubMed: 21047622]

Hortsch, M.; Umemori, H. The Sticky Synapse: Cell Adhesion Molecules and Their Role in Synapse Formation and Maintenance. Springer; New York: 2009.

Kalueff AV, Olivier JD, Nonkes LJ, Homberg JR. Conserved role for the serotonin transporter gene in rat and mouse neurobehavioral endophenotypes. Neurosci Biobehav Rev. 2010; 34:373–386. [PubMed: 19698744]

Katori S, Hamada S, Noguchi Y, Fukuda E, Yamamoto T, Yamamoto H, Hasegawa S, Yagi T. Protocadherin-alpha family is required for serotonergic projections to appropriately innervate target brain areas. J Neurosci. 2009; 29:9137–9147. [PubMed: 19625505]

Kim SY, Yasuda S, Tanaka H, Yamagata K, Kim H. Non-clustered protocadherin. Cell Adh Migr. 2011; 5:97–105. [PubMed: 21173574]

Lander E, Kruglyak L. Genetic dissection of complex traits: guidelines for interpreting and reporting linkage results. Nat Genet. 1995; 11:241–247. [PubMed: 7581446]

Lesch KP, Bengel D, Heils A, Sabol SZ, Greenberg BD, Petri S, Benjamin J, Muller CR, Hamer DH, Murphy DL. Association of anxiety-related traits with a polymorphism in the serotonin transporter gene regulatory region. Science. 1996; 274:1527–1531. [PubMed: 8929413]

Morishita H, Yagi T. Protocadherin family: diversity, structure, and function. Curr Opin Cell Biol. 2007; 19:584–592. [PubMed: 17936607]

Mozhui K, Karlsson RM, Kash TL, Ihne J, Norcross M, Patel S, Farrell MR, Hill EE, Graybeal C, Martin KP, Camp M, Fitzgerald PJ, Ciobanu DC, Sprengel R, Mishina M, Wellman CL, Winder DG, Williams RW, Holmes A. Strain differences in stress responsivity are associated with divergent amygdala gene expression and glutamate-mediated neuronal excitability. J Neurosci. 2010; 30:5357–5367. [PubMed: 20392957]

Murphy DL, Lesch KP. Targeting the murine serotonin transporter: insights into human neurobiology. Nat Rev Neurosci. 2008; 9:85–96. [PubMed: 18209729]

Murphy DL, Fox MA, Timpano KR, Moya PR, Ren-Patterson R, Andrews AM, Holmes A, Lesch KP, Wendland JR. How the serotonin story is being rewritten by new gene-based discoveries principally related to SLC6A4, the serotonin transporter gene, which functions to influence all cellular serotonin systems. Neuropharmacology. 2008; 55:932–960. [PubMed: 18824000]

Myers A, Holmans P, Marshall H, et al. Susceptibility locus for Alzheimer's disease on chromosome 10. Science. 2000; 290:2304–2305. [PubMed: 11125144]

O'Rourke NA, Weiler NC, Micheva KD, Smith SJ. Deep molecular diversity of mammalian synapses: why it matters and how to measure it. Nat Rev Neurosci. 2012; 13:365–379. [PubMed: 22573027]

Ozaki N, Goldman D, Kaye WH, Plotnicov K, Greenberg BD, Lappalainen J, Rudnick G, Murphy DL. Serotonin transporter missense mutation associated with a complex neuropsychiatric phenotype. Mol Psychiatry. 2003; 8:933–936. [PubMed: 14593431]

Perez-Torrado R, Yamada D, Defossez PA. Born to bind: the BTB protein-protein interaction domain. Bioessays. 2006; 28:1194–1202. [PubMed: 17120193]

Poulopoulos A, Aramuni G, Meyer G, Soykan T, Hoon M, Papadopoulos T, Zhang M, Paarmann I, Fuchs C, Harvey K, Jedlicka P, Schwarzacher SW, Betz H, Harvey RJ, Brose N, Zhang W, Varoqueaux F. Neuroligin 2 drives postsynaptic assembly at perisomatic inhibitory synapses through gephyrin and collybistin. Neuron. 2009; 63:628–642. [PubMed: 19755106]

Ramamoorthy S, Bauman AL, Moore KR, Han H, Yang-Feng T, Chang AS, Ganapathy V, Blakely RD. Antidepressantand cocaine-sensitive human serotonin transporter: molecular cloning, expression, and chromosomal localization. Proc Natl Acad Sci U S A. 1993; 90:2542–2546. [PubMed: 7681602]

Ramamoorthy S, Shippenberg TS, Jayanthi LD. Regulation of monoamine transporters: role of transporter phosphorylation. Pharmacol Ther. 2011; 129:220–238. [PubMed: 20951731]

Rao NP, Danivas V, Venkatasubramanian G, Behere RV, Gangadhar BN. Comorbid bipolar disorder and Usher syndrome. Prim Care Companion J Clin Psychiatry. 2010; 12:PCC.09l00792. [PubMed: 20694130]

Rijavec N, Grubic VN. Usher syndrome and psychiatric symptoms: a challenge in psychiatric management. Psychiatr Danub. 2009; 21:68–71. [PubMed: 19270624]

Rioux JD, Xavier RJ, Taylor KD, et al. Genome-wide association study identifies new susceptibility loci for Crohn disease and implicates autophagy in disease pathogenesis. Nat Genet. 2007; 39:596–604. [PubMed: 17435756]

Rottach KG, Schaner BM, Kirch MH, Zivotofsky AZ, Teufel LM, Gallwitz T, Messer T. Restless legs syndrome as side effect of second generation antidepressants. J Psychiatr Res. 2008; 43:70–75. [PubMed: 18468624]

Schmittgen TD, Livak KJ. Analyzing real-time PCR data by the comparative C(T) method. Nat Protoc. 2008; 3:1101–1108. [PubMed: 18546601]

Soiza-Reilly M, Anderson WB, Vaughan CW, Commons KG. Presynaptic gating of excitation in the dorsal raphe nucleus by GABA. Proc Natl Acad Sci U S A. 2013; 110:15800–15805. [PubMed: 24019494]

Sorte HS, Gjevik E, Sponheim E, Eiklid KL, Rodningen OK. Copy number variation findings among 50 children and adolescents with autism spectrum disorder. Psychiatr Genet. 2013; 23:61–69. [PubMed: 23277134]

Steiner JA, Carneiro AM, Blakely RD. Going with the flow: trafficking-dependent and -independent regulation of serotonin transport. Traffic. 2008; 9:1393–1402. [PubMed: 18445122]

Stevens RJ, Akbergenova Y, Jorquera RA, Littleton JT. Abnormal synaptic vesicle biogenesis in Drosophila synaptogyrin mutants. J Neurosci. 2012; 32:18054–18067. 18067a. [PubMed: 23238721]

Sudhof TC. Neuroligins and neurexins link synaptic function to cognitive disease. Nature. 2008; 455:903–911. [PubMed: 18923512]

Sun C, Cheng MC, Qin R, Liao DL, Chen TT, Koong FJ, Chen G, Chen CH. Identification and functional characterization of rare mutations of the neuroligin-2 gene (NLGN2) associated with schizophrenia. Hum Mol Genet. 2011; 20:3042–3051. [PubMed: 21551456]

Sutcliffe JS, Delahanty RJ, Prasad HC, McCauley JL, Han Q, Jiang L, Li C, Folstein SE, Blakely RD. Allelic heterogeneity at the serotonin transporter locus (SLC6A4) confers susceptibility to autism and rigid-compulsive behaviors. Am J Hum Genet. 2005; 77:265–279. [PubMed: 15995945]

Varoqueaux F, Aramuni G, Rawson RL, Mohrmann R, Missler M, Gottmann K, Zhang W, Sudhof TC, Brose N. Neuroligins determine synapse maturation and function. Neuron. 2006; 51:741–754. [PubMed: 16982420]

Veenstra-VanderWeele J, Muller CL, Iwamoto H, Sauer JE, Owens WA, Shah CR, Cohen J, Mannangatti P, Jessen T, Thompson BJ, Ye R, Kerr TM, Carneiro AM, Crawley JN, Sanders-Bush E, McMahon DG, Ramamoorthy S, Daws LC, Sutcliffe JS, Blakely RD. Autism gene variant causes hyperserotonemia, serotonin receptor hypersensitivity, social impairment and repetitive behavior. Proc Natl Acad Sci U S A. 2012; 109:5469–5474. [PubMed: 22431635]

Visscher PM, Thompson R, Haley CS. Confidence intervals in QTL mapping by bootstrapping. Genetics. 1996; 143:1013–1020. [PubMed: 8725246]

Voyiaziakis E, Evgrafov O, Li D, et al. Association of SLC6A4 variants with obsessive-compulsive disorder in a large multicenter US family study. Mol Psychiatry. 2011; 16:108–120. [PubMed: 19806148]

Watson, C.; Paxinos, G. Chemoarchitectonic Atlas of the Mouse Brain. Academic; London: 2010.

Xiong W, Grillet N, Elledge HM, Wagner TF, Zhao B, Johnson KR, Kazmierczak P, Muller U. TMHS Is an integral component of the mechanotransduction machinery of cochlear hair cells. Cell. 2012; 151:1283–1295. [PubMed: 23217710]

Ye R, Blakely RD. Natural and engineered coding variation in antidepressant-sensitive serotonin transporters. Neuroscience. 2011; 197:28–36. [PubMed: 21893166]

Ye H, Liu J, Wu JY. Cell adhesion molecules and their involvement in autism spectrum disorder. Neurosignals. 2010; 18:62–71. [PubMed: 21212702]

Ye R, Carneiro AM, Airey DC, Sanders-Bush E, Williams RW, Lu L, Wang J, Zhang B, Blakely RD. Evaluation of heritable determinants of blood and brain serotonin homeostasis using recombinant inbred mice. Genes Brain Behav. 2014; 13:247–260. [PubMed: 24102824]

Zhu CB, Lindler KM, Campbell NG, Sutcliffe JS, Hewlett WA, Blakely RD. Colocalization and regulated physical association of presynaptic serotonin transporters with A(3) adenosine receptors. Mol Pharmacol. 2011; 80:458–465. [PubMed: 21705486]

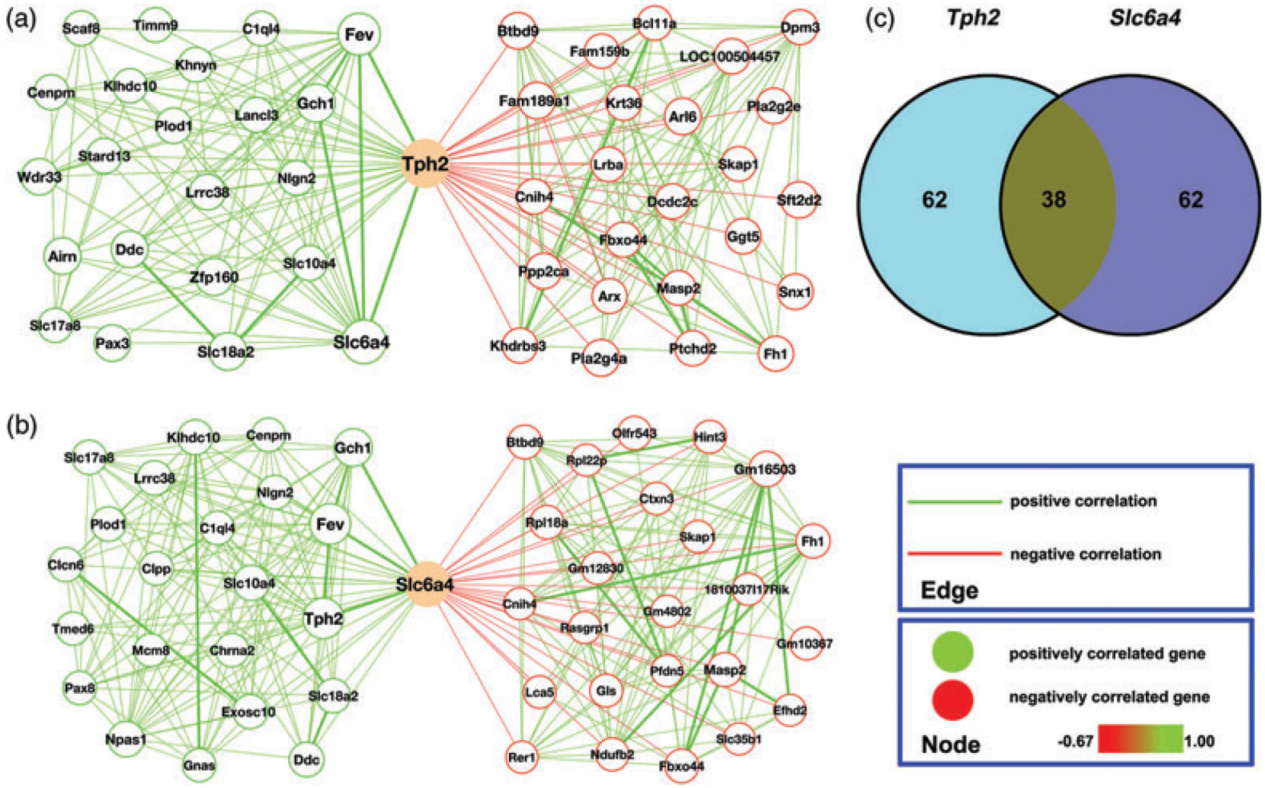

Figure 1. Gene expression networks associated with determinants of midbrain SERT and TPH2 mRNA

Genes (top 25) with highest correlations with *Slc6a4* (a) or *Tph2* (b) are graphed separately based on the direction of correlation (green: positive; red: negative). Gene node sizes represent the significance of correlation. Gene pairs with correlation coefficients (Spearman rho) above 0.5 are connected by edges (green: positive; red: negative). (c) Venn diagram showing the number of overlapping genes derived from *Tph2*-seeded and *Slc6a4*-seeded gene networks (top 100).

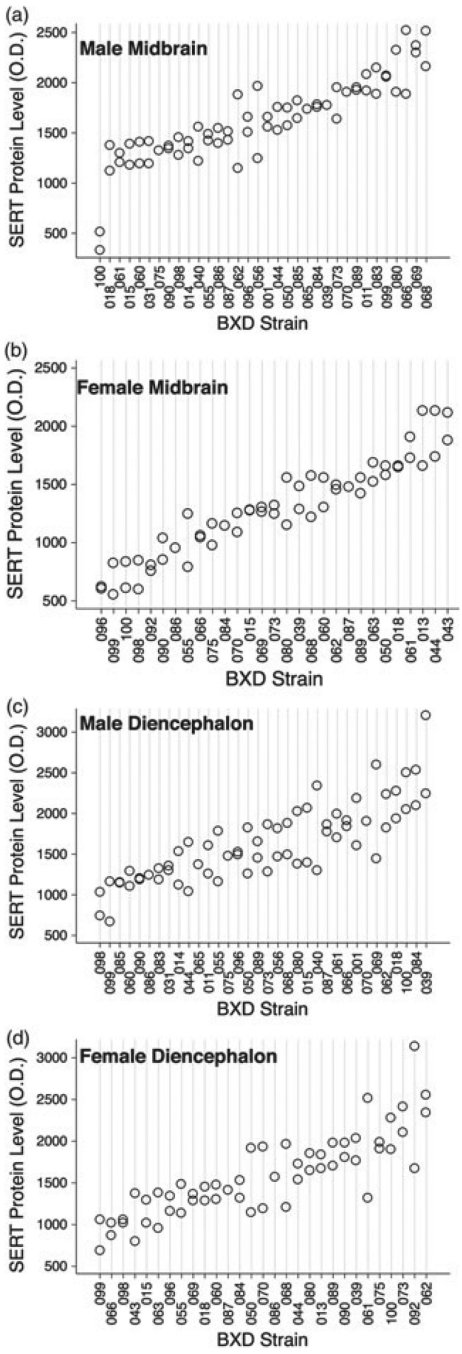

Figure 2. Levels of SERT protein levels across BXD RI lines

(a) Male midbrain; (b) female midbrain; (c) male diencephalon and (d) female diencephalon. Each point represents an individual mouse.

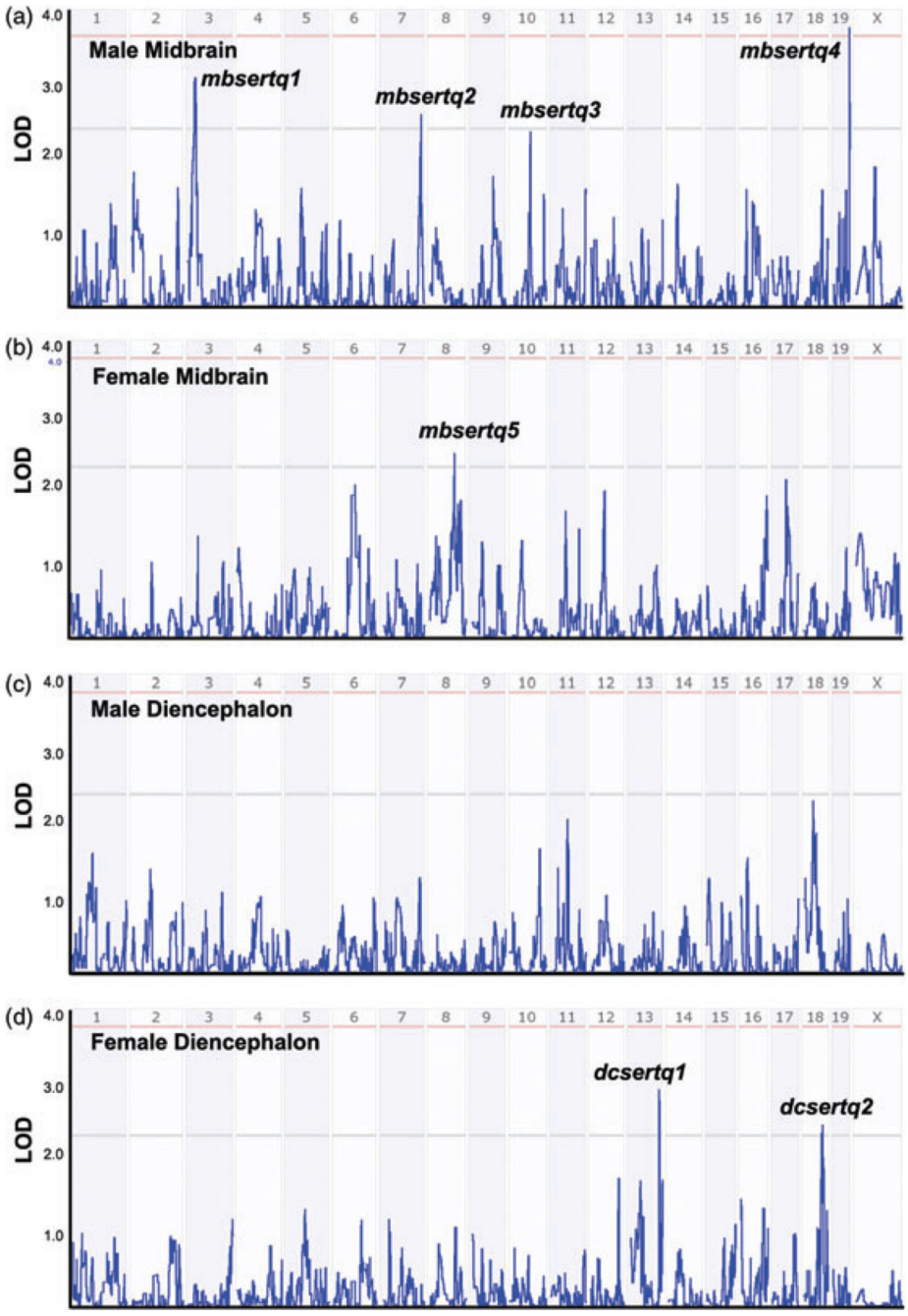

Figure 3. Interval analysis of SERT protein expression levels

(a) Male midbrain; (b) female midbrain; (c) male diencephalon and (d) female diencephalon. Numbers above red lines designate mouse chromosomes. Red lines designate LOD scores where gene variation achieves significance, whereas gray lines designate LOD scores achieving suggestive threshold (see *Materials and methods*).

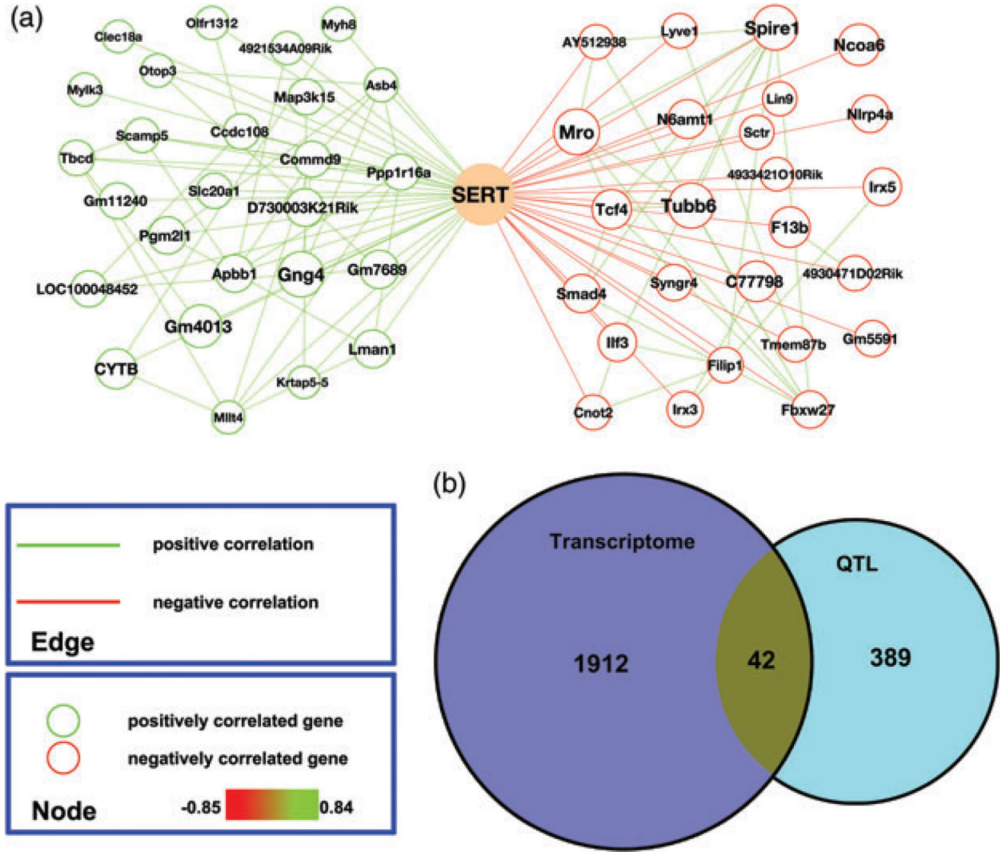

Figure 4. Gene expression networks associated with male midbrain SERT protein expression levels

(a) Genes (top 25) with highest correlations with SERT protein levels are graphed separately based on the direction of correlation (green: positive; red: negative). Gene node sizes represent the significance of correlation. Gene pairs with correlation coefficients (Spearman rho) above 0.5 are connected by edges (green: positive; red: negative). (b) Venn diagram showing the number of total genes and overlapping genes derived from midbrain SERT gene networks and interval mapping of male midbrain SERT protein levels.

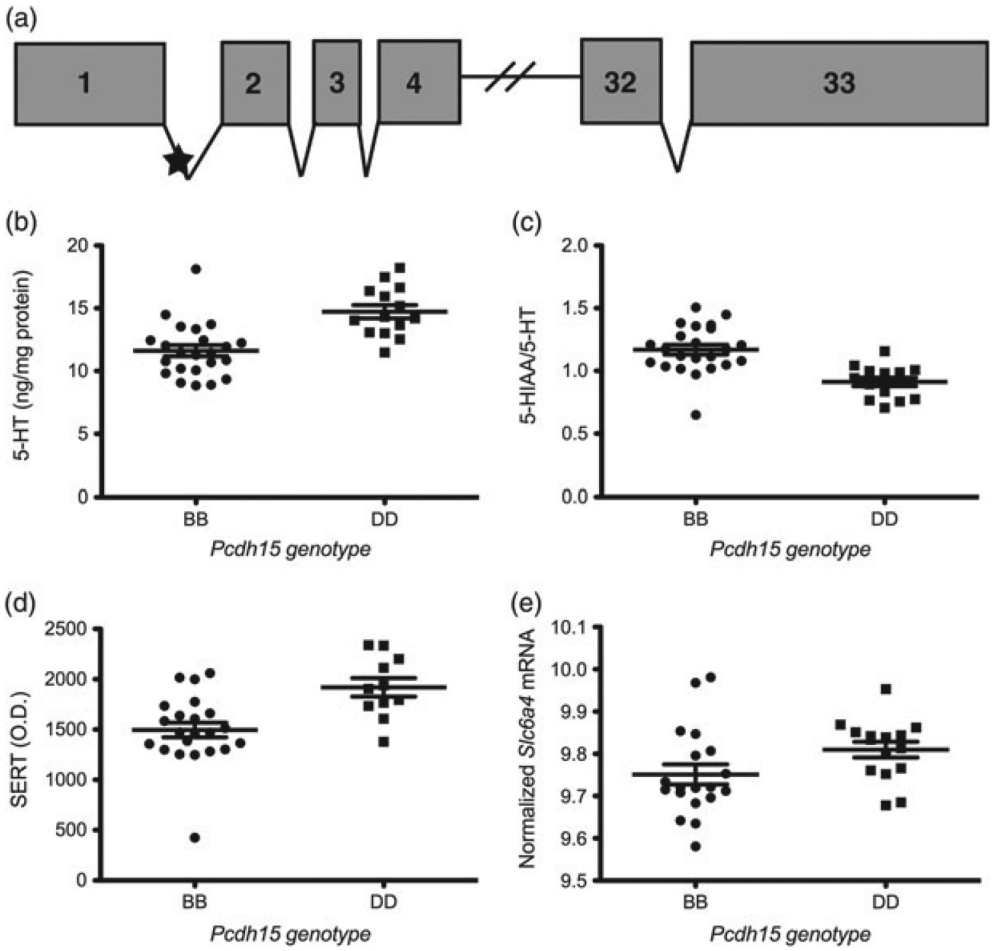

Figure 5. *Pcdh15* SNP rs13480650 is associated with multiple serotonergic traits in BXD RI strains

(a) Genomic structure of mouse *Pcdh15*. Numbers represent exons. Star denotes the location of rs13480650. (b–e) Serotonergic traits are plotted based on the genotype of rs13480650 in BXD strains (5-HT: $P < 0.0001$; 5-HIAA/5-HT: $P < 0.0001$; SERT: $P < 0.01$; *Slc6a4*: $P < 0.05$). All P values are calculated using Student's t-test.

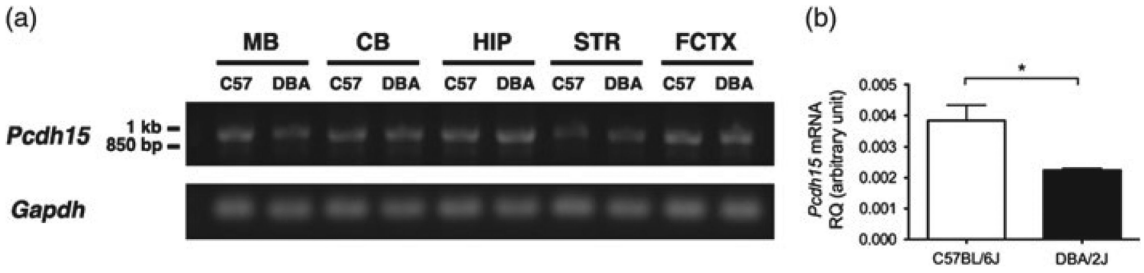

Figure 6. Characterization of *Pcdh15* expression in the mouse brain by RT-PCR

(a) PCR products amplified from *Pcdh15* cDNA of multiple brain regions in C57BL/6J (C57) and DBA/2J (DBA) mice. MB, midbrain; CB, cerebellum; HIP, hippocampus; STR, striatum; FCTX, frontal cortex. (b) C57BL/6J mice have higher *Pcdh15* expression in the midbrain than DBA/2J, measured by qPCR ($P < 0.05$, Student's *t*-test).

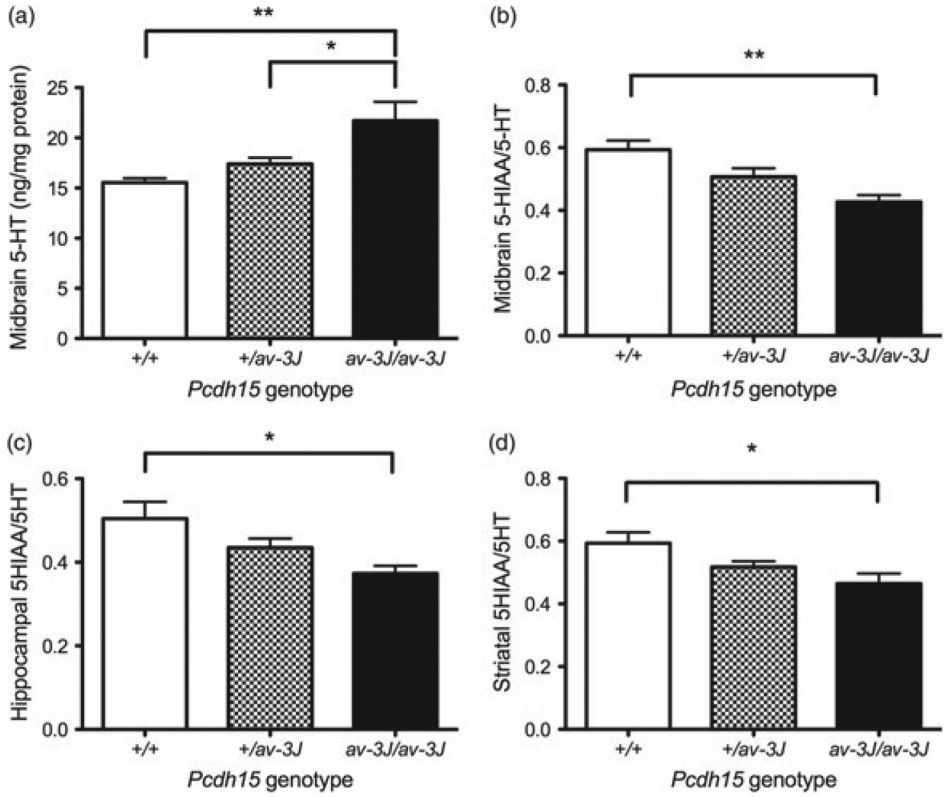

Figure 7. ***Pcdh15*$^{av\text{-}3J}$ mice have altered brain 5-HT traits**

(a) Midbrain 5-HT levels ($P < 0.01$); (b) midbrain 5-HT turnover ratios ($P < 0.01$); (c) hippocampal 5-HT turnover ratios ($P < 0.05$) and (d) striatal 5-HT turnover ratios ($P < 0.01$). All P values are calculated using Kruskal–Wallis test. Significance noted on pairwise comparisons is calculated using Dunn's multiple comparison tests. N = 5–7 (wt), 16–25 (het) and 8–12 (hom).

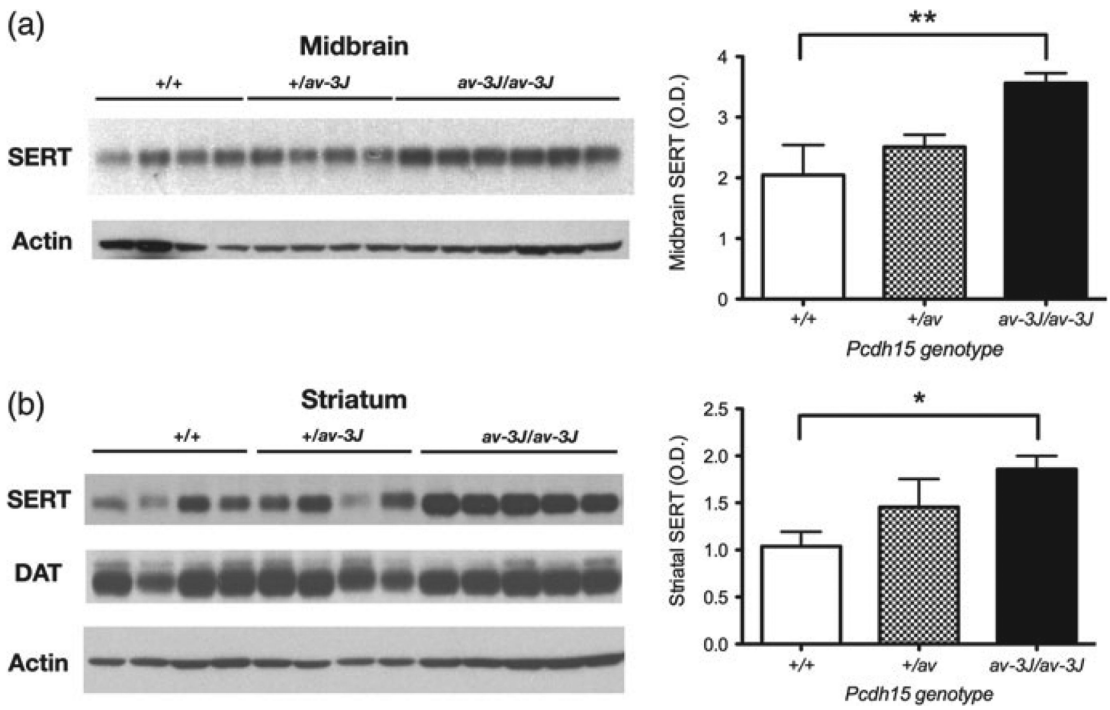

Figure 8. *Pcdh15*$^{av\text{-}3J}$ mice have elevated SERT protein expression levels

(a) Midbrain ($P < 0.01$) and (b) striatum ($P < 0.05$). *P* values are calculated using one-way ANOVA followed by Bonferroni's multiple comparison tests.

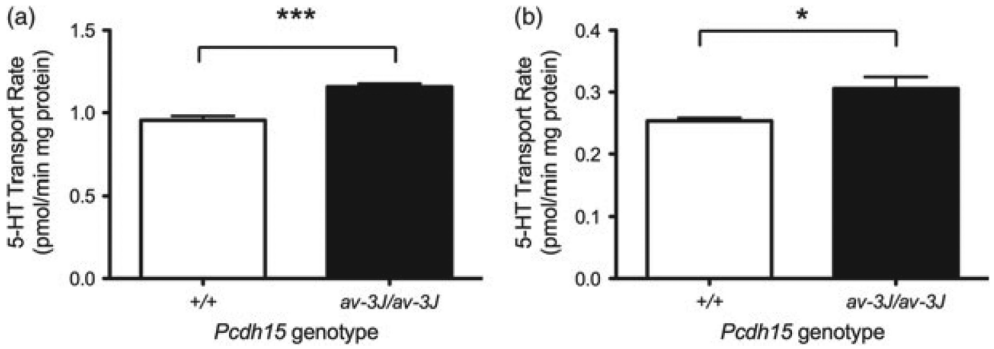

Figure 9. *Pcdh15*$^{av\text{-}3J}$ mice have increased 5-HT synaptosomal uptake

(a) Midbrain ($P < 0.001$) and (b) hippocampus ($P < 0.05$). P values are calculated using Student's t-test. $N = 4$ for each genotype.